AMERICAN ACADEMY OF OPHTHALMOLOGY®

Rapid Objective Testing of Visual Function Matched to the ETDRS Grid and Its Diagnostic Power in Age-Related Macular Degeneration

Bhim B. Rai, MD, PhD,[1,2] *Faran Sabeti, BOptom, PhD,*[1,3] *Corinne F. Carle, PhD,*[1] *Emilie M. Rohan, MOrth,*[1] *Josh P. van Kleef, PhD,*[1] *Rohan W. Essex, MBBS, FRANZCO,*[4] *Richard C. Barry, MBBS, FRANZCO,*[5] *Ted Maddess, PhD*[1]

Purpose: To study the power of an 80-second multifocal pupillographic objective perimetry (mfPOP) test tailored to the ETDRS grid to diagnose age-related macular degeneration (AMD) by Age-Related Eye Disease Study (AREDS) severity grade.

Design: Evaluation of a diagnostic technology.

Methods: We compared diagnostic power of acuity, ETDRS grid retinal thickness data, new 80-second M18 mfPOP test, and two wider-field 6-minute mfPOP tests (Macular-P131, Widefield-P129). The M18 stimuli match the size and shape of bifurcated ETDRS grid regions, allowing easy structure−function comparisons. M18, P129, and P131 stimuli test both eyes concurrently. We recruited 34 patients with early-stage AMD with a mean ± standard deviation (SD) age of 72.6 ± 7.06 years. The M18 and P129 plus P131 stimuli had 26 and 51 control participants, respectively with mean ± SD ages of 73.1 ± 8.17 years and 72.1 ± 5.83 years, respectively. Multifocal pupillographic objective perimetry testing used the Food and Drug Administration-cleared Objective FIELD Analyzer (OFA; Konan Medical USA).

Main Outcome Measures: Percentage area under the receiver operator characteristic curve (AUC) and Hedge's g effect size.

Results: Acuity and OCT ETDRS grid thickness and volume produced reasonable diagnostic power (percentage AUC) for AREDS grade 4 eyes at 83.9 ± 9.98% and 90.2 ± 6.32% (mean ± standard error), respectively, but not for eyes with less severe disease. By contrast, M18 stimuli produced percentage AUCs from 72.8 ± 6.65% (AREDS grade 2) to 92.9 ± 3.93% (AREDS grade 4), and 82.9 ± 3.71% for all eyes. Hedge's g effect sizes ranged from 0.84 to 2.32 (large to huge). Percentage AUC for P131 stimuli performed similarly and for P129 performed somewhat less well.

Conclusions: The rapid and objective M18 test provided diagnostic power comparable with that of wider-field 6-minute mfPOP tests. Unlike acuity or OCT ETDRS grid data, OFA tests produced reasonable diagnostic power in AREDS grade 1 to 3 eyes. *Ophthalmology Science 2022;2:100143* © *2022 by the American Academy of Ophthalmology. This is an open access article under the CC BY-NC-ND license (http://creativecommons.org/licenses/by-nc-nd/4.0/).*

Supplemental material available at www.ophthalmologyscience.org.

Age-related macular degeneration (AMD) continues to be a leading cause of irreversible blindness and visual impairment worldwide both in developed[1,2] and developing[3–5] countries. It poses a public health burden compromising social, physical, and emotional well-being and demands effective and early intervention.[6,7]

Measuring retinal thickness with OCT is now a standard procedure. However, thickness is poorly correlated with functional change.[8] The most common clinical end point in AMD studies is best-corrected visual acuity (BCVA). A major issue with BCVA is that it is a measure of the function of just the central fovea, and a sight-threatening lesion may be expanding nearby and may not be picked up by BCVA measurement. Historically, visual acuity has been a surrogate of sight-threatening structural changes in the macula; however, it is now well established that retinal changes can precede changes in BCVA, although other functional vision tests, including blue-cone function, dark adaptation, and flicker perimetry, largely detect only late-stage AMD.[9]

Multifocal pupillographic objective perimetry (mfPOP) assesses both sensitivity and response delay at each of many visual field locations of both eyes simultaneously. The method is very similar to a dichoptic multifocal visual

https://doi.org/10.1016/j.xops.2022.100143
ISSN 2666-9145/22

evoked potential (mfVEP) using 2 scalp electrodes, but where the time-varying diameters of the 2 pupils are substituted for the 2 evoked electrical responses. As in an mfVEP, independent stimuli are presented concurrently to many different visual field locations. Like a 2-electrode mfVEP, the 2 pupils each record activity from both retinas. Several anatomic studies show that the pretectal olivary nuclei derive substantial input from the extra-striate cortex.[10] Head-to-head mfVEP and mfPOP studies on the same participants also showed that unique features of mfPOP responses are recorded on electroencephalography electrodes that obtain their drive from the extra-striate cortex.[11]

We have published 5 studies of evolving variants of mfPOP in AMD showing good diagnostic power in all disease stages.[9,11–14] In the present study, mfPOP was undertaken using a Food and Drug Administration-cleared prototype Objective FIELD Analyser (OFA; Konan Medical USA). Current perimetry methods are spatially mismatched to current structural test patterns. Therefore, we designed an 80-second OFA test, the M18 protocol, which has test stimuli that map directly to the ETDRS grid to allow direct comparisons between structure and function of the macula. In this study, we correlated OCT ETDRS grid data and M18 functional outcomes for early- to late-stage AMD. We also compared 2 published 6-minute OFA tests with the M18 protocol. All 3 OFA methods tested both eyes concurrently. We compared the diagnostic power outcomes of the OFA tests with those for BCVA and OCT ETDRS grid thickness and volume data.

Methods

Participants

We recruited 34 patients (9 men) with early- to late-stage AMD: Age-Related Eye Disease Study (AREDS) stages 1 to 4.[15] The M18 study (see stimuli below) included 26 control participants (10 men). Mean ± standard deviation (SD) ages were 72.6 ± 7.06 years for patients and 73.1 ± 8.17 years for control participants. For the P129 and P131 studies, the same patients participated, and we obtained normative data for 51 participants (23 men) 72.1 ± 5.83 years of age. Age range for both studies was 62 to 90 years. We excluded participants who had ophthalmologic or neurologic diseases other than AMD that would potentially affect visual acuity, color vision, visual fields, or pupillary function; cataract of more than grade 3 nuclear sclerosis according to the Lens Opacification Classification System III or media opacities; trauma to eyes or head; or systemic diseases such as diabetes and hypertension. We also excluded patients who had undergone uncomplicated cataract surgery within 6 months and complicated cataract surgery at any time. The Australian National University Ethics Committee and Australian Capital Territory Health Ethics Committee approved the study, and informed written consent was obtained from all participants. The research adhered to the tenets of the Declaration of Helsinki.

Ophthalmic Examinations

The participants underwent comprehensive anterior and posterior segment evaluations. We performed 10-2 visual field testing with the Matrix perimeter (Carl Zeiss Meditec, Inc), measured BCVA using ETDRS charts, carried out slit-lamp examination to rule out pupillary abnormality and media opacity, and measured intraocular pressure with Goldmann applanation tonometry. We also undertook pachymetry (Pachmate DGH 55; DGH Technology Inc) and corneal curvature (ARK-1s; NIDEK Co. Ltd) analysis. Pupils were dilated with 1% tropicamide eye drops. Macular scanning producing both 8 × 8 grid data and 9 ETDRS grid data, as well as retinal nerve fiber layer data, were performed with a Spectralis OCT device (Heidelberg Engineering GmbH). Macular color photographs, normal and magnified ×2, were obtained (CR-2 digital retinal camera; Canon, Inc). These color fundus photographs were used for AMD grading by 2 retinal specialists (B.B.R. and R.W.E.) based on the AREDS system.[15]

Stimuli—Multifocal Pupillographic Objective Perimetry

Multifocal pupillographic objective perimetry was performed before any other eye tests on the day to reduce confounding factors, particularly pupil dilation.[16] The participants did not drink caffeinated beverages within 1 hour of the test. Presentation of stimuli and real-time monitoring of the pupil diameter with infrared video cameras was carried out using a Food and Drug Administration-cleared prototype OFA mfPOP device. It concurrently presents independent multifocal stimuli to both eyes while measuring direct and consensual responses from every visual field location stimulated (Fig 1).[17] Details of the analysis are given elsewhere.[18,19]

We compared 3 OFA stimulus variants (Fig 2A–D). Two were older 6-minute stimuli named P129 and P131. P129 has a widefield stimulus array with 44 test regions covering the central 60° of the visual field (Fig 2A, B). P131 is a macular version having all its elements scaled by half compared with P129, so that its 44 stimuli cover the central 30° (Fig 2C). Our published mfPOP studies of retinal disease indicate that P131 has higher diagnostic value in retinal disease than P129.[20] We introduced a new 80-second variant, M18 (Fig 2D), which matches the ETDRS grid, with 2 stimuli per ETDRS grid sector (Fig 2E, F). Patients were tested with the 3 protocols in the same session in randomized order.

Statistical Analysis

Matlab software version 2016b (The MathWorks) was used for data analysis. The response waveforms for each of the 18 or 44 test regions per eye were extracted from raw pupillary responses using a multiple regression method.[21–23] The average response waveforms for each retinal region were fitted to a log-normal function,[24] allowing per-region constriction amplitude (sensitivity) and time to peak (delay), to be measured. The regressive method generated standard errors for all the estimated constriction amplitudes and delays, that is, time to peak of the constriction.[17,18] We normalized amplitudes, greatly reducing the effect of age, but herein report only response delays.

The normative models for each method were simply the medians at each test region of all the control eyes. Before calculating the medians, the per-region data from right eyes were reflected to the left-eye equivalent locations. Thus, the normative data from anatomically equivalent pairs of regions in the 2 eyes of each participant were combined.

For the receiver operating characteristic (ROC) curve analysis, we examined the per-region response amplitudes (transformed to decibel sensitivity) and delays, but report only the latter herein. For each of those, we calculated the standard perimetry measures: total deviations (TDs) and pattern deviations (PDs), and we also examined per-region asymmetries between the 2 eyes. The TDs are simply the per-region differences from the normative data. The PDs are derived from the TDs by taking the 86th percentile of the TD data, an approximation of data from undamaged parts of the field,

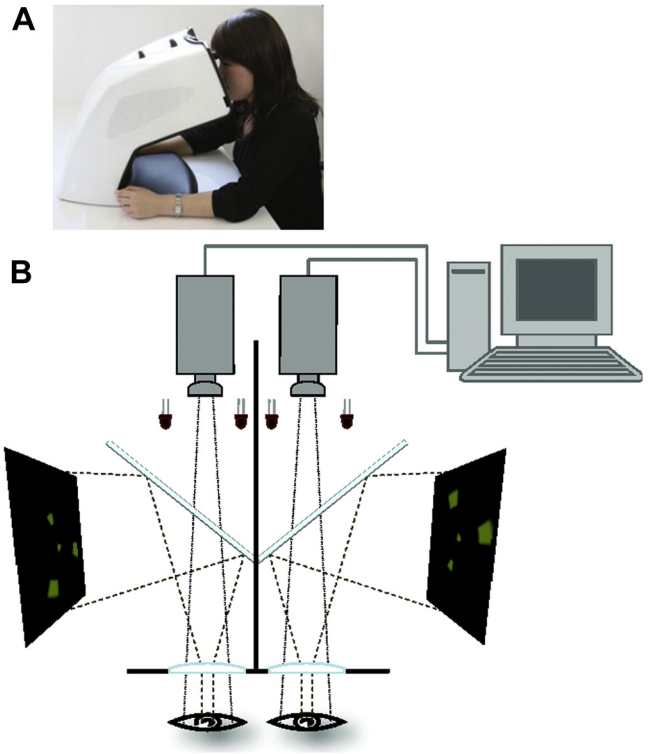

Figure 1. The Objective FIELD Analyser (OFA) device. **A**, Illustration of a test participant seated and looking into the OFA objective lenses. **B**, Diagram showing the dichoptic stimulus arrangement inside the OFA. The pseudorandomly sequenced brief-onset stimuli are presented on 2 displays. Cold mirrors direct the eyes to the 2 displays. Infrared video cameras capture images of the 2 pupils. The record of the pupil diameters and the stimulus histories are used to extract the responses to each of the up to 44 stimulus test regions per eye. See Figure 2.

and subtracting that from the TDs to yield a within-subject control. As is often the case in perimetry, the best results were obtained for the PDs, so we restrict ourselves to those data in the interest of space.

We considered an alternative delay measure: the absolute value of the differences from normal delays (abs(DelayDiff)). Our previous mfPOP studies indicate that earlier-stage AMD is often characterized by quicker than normal delays.[12,13] The suggested reason is upregulation of retinal activity in response to disease, which later fails to compensate for damage, leading to longer than normal delays in later-stage disease.

The severity of disease in the participants was based on the AREDS 4-step scale.[15] Stage 4 is characterized by either geographic atrophy or exudative AMD. Among the 68 patient eyes, the distribution of eyes per AREDS step was: AREDS step 1, 28 eyes; AREDS step 2, 18 eyes; AREDS step 3, 13 eyes; and AREDS step 4, 9 eyes. The 9 AREDS step 4 eyes all showed exudative AMD. Using ROC curve analysis, we quantified the ability to differentiate eyes of different AREDS steps from control eyes. Additionally, we performed ROC curve analyses comparing control eyes with AMD eyes from pooled groups of AREDS steps, including all eyes, to examine percentage area under the ROC curve (AUC) estimates from larger numbers of eyes.

For the OFA and OCT data, we used our standard ROC analysis method of recomputing the percentage AUC for each of the means of selections of the N worst (most deviating from normal) regions. Examining how percentage AUC changes with respect to differing numbers of damaged regions averaged provides an indication of the number of regions appearing in the measured visual field data that are diagnostic. All models excluded the single worst region of every field or OCT scan. Because some analyses considered smaller numbers of eyes, we kept our normative models very simple. Models adjusted for age provided percentage AUC values that were a few percent better, but we decided to be conservative. Models adjusting for sex made no difference. As an alternative way of indicting diagnostic power, we report effect-size calculated as Hedge's g, which is Cohen's d corrected for smaller sample sizes.

For the OCT scans, the normative data was the median at each region of the control eyes with right-eye data reflected to produce left-eye equivalents. For comparison, we took the means of 3 published normative ETDRS grid retina thickness data sets[25–27] and found that the per-region means differed from our normative data by only 1.19 ± 0.2 μm (mean ± SD).

Results

Best-Corrected Visual Acuity and OCT ETDRS Grid Measures

Given the very common use of BCVA to manage AMD patients, we examined the percentage AUC (± standard error) for BCVA for the 4 AREDS severities (Table 1). We also computed percentage AUC values for the 9-region ETDRS retinal thickness and volume data. We repeated that analysis for the per-region thickness and volumes, as well as log-transformed versions (in case the diagnostically relevant measure was n-fold change). We found that log volumes outperformed the volumes themselves, and so only report those in Table 1. We examined both TDs and PDs (see "Methods"). We report PDs here because they performed better than the simple deviations from normal (TDs), and PDs were also used for the OFA data (see below). The reported AUC values for the OCT data are for the of mean worst 2 regions (most differing from normative) in each ETDRS grid data set. The 2 worst regions provided the best performance. Like BCVA, the only useful diagnostic power was for AREDS 4 eyes, with percentage AUCs of approximately 90%.

M18 Test

Per-region sensitivities of the M18 test showed less diagnostic usefulness than per-region delays. Therefore, we present delay data here. The left 2 columns give the percentage AUC ± standard error for the per-region response delays (rows 1–4) and the abs(DelayDiff) (rows 5–8). The column labels n = 3 and n = 9 indicate the number of n-worst regional delays averaged to provide data for each ROC analysis. Given that M18 has 18 regions per eye, n = 3 indicates the mean of worst one-sixth of regions and n = 9 indicates half the regions. The right 2 columns give the Hedge's g values, quantifying effect size. The standards for Hedge's g effect sizes of small, medium, large, very large,

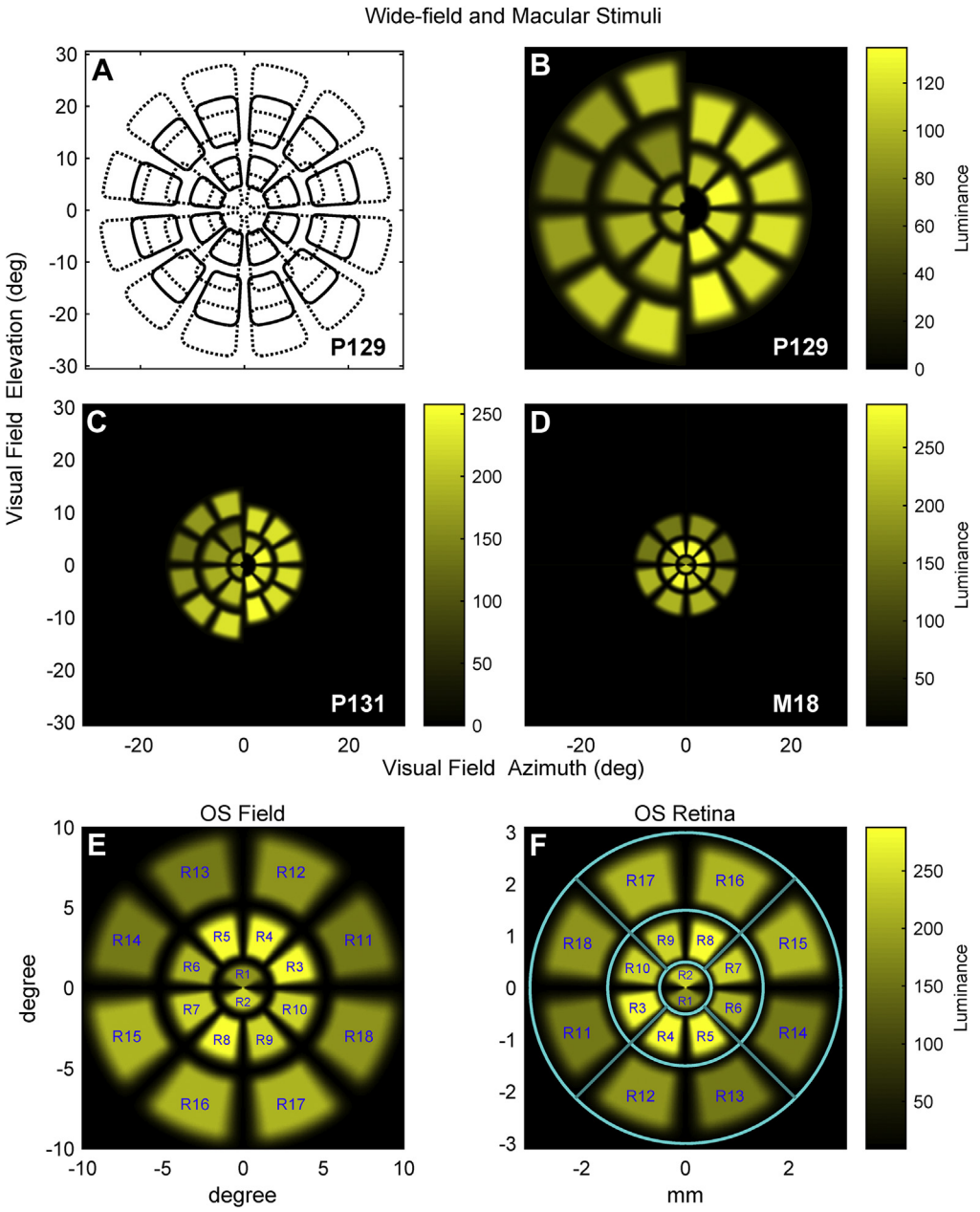

Figure 2. Representations of the 3 Objective FIELD Analyser (OFA) stimulus types. All stimuli shown are those for the left eye (OS); stimuli for the right eye (OD) were mirror image. **A**, Contours of the 44 stimulus regions of the widefield P129 stimulus. The transiently presented (33 ms) stimuli were delivered pseudorandomly, with a mean per-region interval of 4 s. In practice, overlapping regions are never presented concurrently. **B**, Stimuli from the left and right halves of the 5 rings of P129 stimuli showing their relative intensities. **C**, Same as for (**B**), but for the 44-region P131 macular stimulus array. **D**, M18 stimulus array. **E**, Numbering scheme of the M18 stimuli as presented in visual space to OS. **F**, The projection of the M18 stimuli onto the retina showing the relationship to the ETDRS grid (cyan).

and huge are 0.2, 0.5, 0.8, 1.2, and 2.0. Most of the g values in Table 2 are in the very large to huge range.

The AREDS grade 1 group is surprisingly robust, especially when the abs(DelayDiff) measure is used, producing percentage AUC values of 85.1 ± 4.44% for the mean of the 9-worst performing regions. That was better than the BCVA for AREDS grade 4, as are the values for AREDS grade 3, where values for delay were 86.8 ± 5.33%. The values of 92.9 ± 3.93% and Hedge's g of > 2 for delays in AREDS grade 4 eyes are exceptional. We also recomputed the percentage AUC for pooled groups of eyes to obtain more conservative values for larger numbers of eyes (Table 3). Diagnostic power and effect-size remained high.

We further examined correlations between the delay PDs and the OCT data. For that, we calculated means of pairs of

Table 1. Percentage Area under the Receiver Operating Characteristic Curve for Best-Corrected Visual Acuity and OCT 9-Region ETDRS Grid Data

	Age-Related Eye Disease Study Grade			
	1	*2*	*3*	*4*
BCVA	57.6 ± 6.76	42.6 ± 7.77	72.0 ± 7.20	83.9 ± 9.98
Thickness	44.2 ± 7.30	65.4 ± 8.05	54.6 ± 11.8	90.2 ± 7.07
log volume	44.4 ± 7.39	65.3 ± 7.90	49.0 ± 11.9	90.2 ± 6.32

BCVA = best-corrected visual acuity.

M18 per-region data according to the mapping between M18 and the ETDRS grid (Fig 2E, F) to give 9 M18 equivalents per eye. All the correlations were low, with only some correlations of AREDS grade 4 eyes being significant. For thickness, log thickness, and log volumes, the AREDS grade 4 correlations were $r = 0.301$, $r = 0.288$, and $r = 0.288$ ($P = 0.006$, $P = 0.009$, and $P = 0.009$, respectively). The correlations indicate that thicker, or more voluminous, retinal regions are associated with slower per-region OFA delays.

P129 and P131 Tests

For comparison with published studies, we also examined the 6-minute widefield P129 and macular P131 tests. P129 and P131 test larger areas of the retina than M18 (Fig 1A–D), and both test 44 regions of the field. Because of the larger number of regions, we report on larger n worsts of 5 and 15, which in terms of proportion of the field sampled are comparable with 2 and 6 regions for M18.

Delay was better for P131, and abs(DelayDiff) was better for P129 (Table 4). Generally speaking, the results for n = 5 were better for less severe disease, and the results for n = 15 were better for more severe disease. This indicates a larger number of abnormal regions in more severe disease. P129 approached the performance of BCVA in milder disease (Table 1).

Discussion

The importance of rapid diagnostic tests to save time in clinics is imperative to buy time and to deliver standard eye care. In early-stage AMD, despite normal visual acuity, many patients report alterations to visual perception.[28,29] This suggests the significance of considering the functional aspect as eyes progress from early- to late-stage AMD. Scotopic microperimetry is shown to be useful in evaluating early-stage AMD,[30] but the test duration is long, and it needs additional time for dark adaptation. Montesano et al[31] reported that mesopic microperimetry showed better structure–function correlation compared with scotopic microperimetry in patients with macular drusen. However, the relationship was weak, likely because of the early functional damage and small number of tested locations. In our own study, we found similar mfPOP sensitivity and specificity at photopic and scotopic levels, although at photopic levels, the damage was recorded more diffusely across the visual field. We also assessed single-flash versus flicker mfPOP in AMD in that study and a later one,[9,32] but found similar results, as was reported by Luu et al, who compared automated single-flash and flicker perimetry.[33]

For the 80-second M18 OFA test, the per-region response delays showed the best diagnostic power. Perhaps the finer measurement by smaller stimuli is a factor (Fig 2B–D). M18 also performed better, or as well as, the delays of either P129 or P131, both of a 6-minute duration. For the 28 AREDS grade 1 eyes, the delay percentage AUC was 84.3 ± 4.21%, and for abs(DelayDiff), the percentage AUC was 85.1 ± 4.44% (Table 2), both much better than the chance levels of performance for BCVA and the OCT ETDRS grid data (Table 1). All 4 AREDS levels had large to huge Hedge's g effect sizes. Even when all AREDS grade 1 to 3 eyes and grade 1 to 4 eyes were pooled, the g values were 1.74 and 2.56, respectively (Table 3).

The AREDS grade 2 eyes often showed the lowest AUCs, but this may illustrate issues with the AREDS classification

Table 2. Percentage Area under the Receiver Operating Characteristic Curve and Hedge's g Values for Objective FIELD Analyzer M18 Delays

	N Worst Value			
	Percentage Area under the Receiver Operating Characteristic Curve ± Standard Error		*Hedge's g Value*	
	3	*9*	*3*	*9*
Delay				
AREDS Grade 1	83.8 ± 4.38	84.3 ± 4.21	1.24	1.23
AREDS Grade 2	69.1 ± 7.51	72.8 ± 6.65	0.81	0.84
AREDS Grade 3	85.8 ± 5.87	86.8 ± 5.33	1.79	1.83
AREDS Grade 4	91.5 ± 4.56	92.9 ± 3.93	2.32	2.48
abs(DelayDiff)				
AREDS Grade 1	84.7 ± 4.45	85.1 ± 4.44	1.31	1.32
AREDS Grade 2	65.7 ± 7.34	69.8 ± 7.05	0.50	0.62
AREDS Grade 3	81.4 ± 6.97	81.7 ± 7.31	1.35	1.37
AREDS Grade 4	80.3 ± 7.63	79.3 ± 8.56	1.48	1.44

abs(DelayDiff) = delay difference; AREDS = Age-Related Eye Disease Study.

Table 3. Percentage Area under the Receiver Operating Characteristic Curve for Pooled Objective FIELD Analyzer M18 Delays

	N Worst Value			
	Percentage Area under the Receiver Operating Characteristic Curve ± Standard Error		*Hedge's g Value*	
Delay	*3*	*9*	*3*	*9*
AREDS Grade 1–2	78.1 ± 4.58	79.8 ± 4.39	1.24	1.23
AREDS Grade 1–3	79.8 ± 4.12	81.4 ± 4.00	1.79	1.83
AREDS Grade 1–4	81.3 ± 3.81	82.9 ± 3.71	2.32	2.48

AREDS = Age-Related Eye Disease Study.

scheme.[15] Several smaller drusen can be AREDS grade 1, whereas just 1 druse of > 125 μm, or a small pigmentary change (even with no drusen), can switch an eye from AREDS grade 1 to AREDS grade 2. Thus, AREDS is a very nonlinear clinical scale. Table 3 shows that when the AREDS grade 1 and 2 eyes were pooled, percentage AUC was still close to 80%, as we have reported before for P131.[9] Most impressive were the M18 results for AREDS grade 3 eyes at 86.8 ± 5.33% compared with 72.0 ± 7.20% for BCVA and chance performance for the ETDRS measures. Currently, these at-risk patients are managed mainly based on BCVA and OCT findings. That being said, higher-resolution OCT estimates of retinal thickness, like the Spectralis 8 × 8 grid, may provide better performance than ETRDS grid data.[8]

Previously, we reported that asymmetry between anatomically equivalent regions of the 2 eyes can provide high diagnostic power for early-stage AMD.[9,12] Therefore, we repeated the ROC analyses using these between-eye asymmetries. The resulting percentage AUC data for P129 and P131 were better than for M18, especially for P129, suggesting that this diagnostic signal is driven more by the peripheral retina. This is not surprising because we have reported that faster, large peripheral responses are a marker for wet AMD eyes responding well to anti–VEGF treatment.[13] Table 4 indicated that Abs(DelayDiff) was better for P129, again suggesting that faster than normal peripheral responses may be indicative of early-stage functional changes. Although this metric is somewhat unusual, we have reported on it in some detail in recent mfPOP studies of diabetic macular edema and neovascular AMD using P129 and P131.[34,35] Faster responses are also accompanied by hypersensitivity in both diabetic retinopathy and AMD, and these changes are observed for mfPOP and multifocal visual evoked potentials when tested in the same patients on the same day.[11]

From our large normative databases for the wider-field 6-minute OFA tests, we know that small but significant age and sex effects exist. Those were largely ignored herein to produce conservative estimates of percentage AUC and Hedge's g value. It is likely that with normative models produced from larger normative data sets that higher AUC and Hedge's g values will be achieved.

An interesting outcome is that for OCT data, log volume seemed to have higher diagnostic power than volume itself. This may suggest that examining n-fold change in regional volumes is worth pursuing. Log transformation of OCT thickness data has proven useful for other purposes, too.[36]

Age-related macular degeneration is one of the major causes of irreversible blindness both in developed and developing countries.[37] Developing countries have limited human and diagnostic resources, which is further complicated by the unequal distribution of health workers, such that rural regions are often understaffed.[38] Age-related macular degeneration has been a burden in

Table 4. Percentage Area under the Receiver Operating Characteristic Curve for P129 and P131 Delay Measures

	N Worst Value			
	Percentage Area under the Receiver Operating Characteristic Curve ± Standard Error		*Hedge's g Value*	
	5	*15*	*5*	*15*
P129 abs(DelayDiff)				
AREDS Grade 1	67.6 ± 6.60	66.0 ± 6.64	0.70	0.58
AREDS Grade 2	**64.6 ± 7.42**	**59.3 ± 7.65**	**0.59**	**0.39**
AREDS Grade 3	87.2 ± 3.59	86.9 ± 3.61	1.58	1.54
AREDS Grade 4	**83.8 ± 5.21**	**84.7 ± 4.76**	**1.75**	**1.63**
P131 Delay				
AREDS Grade 1	73.9 ± 4.93	72.8 ± 5.13	0.97	0.95
AREDS Grade 2	**73.8 ± 5.71**	**70.6 ± 6.70**	**0.96**	**0.88**
AREDS Grade 3	82.0 ± 5.94	82.9 ± 5.79	1.75	1.74
AREDS Grade 4	**88.5 ± 5.23**	**90.3 ± 4.62**	**2.59**	**2.62**

abs(DelayDiff) = delay difference; AREDS = Age-Related Eye Disease Study. Boldface indicates statistical significance.

developing countries, both in clinics and operating theaters. It is reported that more than half of the registered procedures in operating theaters are for intravitreal injection of anti−vascular endothelial growth factor as part of wet AMD treatment administered in the operating theaters as mandated in some countries.[39] From the above examples, it is clear that the development of an affordable, short-duration diagnostic test would be very useful. Partly for these reasons, we investigated the diagnostic usefulness of the M18 mfPOP test.

Another motivation was to have perimetric stimuli that match the layout of the ubiquitous ETDRS grid. By bifurcating the ETDRS grid regions, the M18 stimuli respect the vertical and horizontal meridians of the retina and field. This could extend the use of M18 to diseases like late-stage glaucoma or posterior-pole stroke, where sparing of central vision by processes that follow the meridians is relevant. Given that OCT signal-to-noise ratios have improved since the ETDRS grid was introduced, it might make sense for manufacturers to provide an M18-like scan with 18 regions. Reporting log-transformed measures also may be useful. Relatively few studies have made point-by-point comparisons of OCT and perimetry data in AMD. This may be because OCT and perimetry devices use different spatial layouts to report their data, requiring complex mapping from one report format to another to permit pointwise comparisons. We and other investigators have demonstrated such transformation methods.[8,40,41] Herein, we obviated the need for transformation by matching our M18 stimuli to the OCT ETDRS grid. The M18 stimuli also reduce another issue for many perimeters, poor reproducibility. Poor reproducibility in part is the result of the very small stimuli they use interacting with sharply varying scotomas, a factor that is reduced by the large smooth-sided M18 stimuli.[42]

This study would be improved by having a larger number of participants. Another potentially valuable investigation would be to examine the sublayers of the ETDRS grid data.[40,41] Mapping the finer-grained Spectralis 8 × 8 posterior pole data onto equivalent M18 regions[8] might provide better correlations between the methods and possibly better diagnostic power for the OCT data.

In conclusion, in terms of diagnostic power, M18 was as good or better than the wider-field, longer-duration OFA tests. Except for AREDS grade 4 eyes, M18 was much better than either BCVA or ETDRS grid OCT data. The wider-field tests confirmed that early-stage disease also produces faster than normal responses in more peripheral retina. In developing countries, it is imperative to have rapid, cost-effective testing permitting limited human resources to evaluate as many patients as possible. M18 may provide that. M18 may also provide clinical end points for the development of new interventions for early AMD or complement methods for pro re nata management of exudative AMD.

Footnotes and Disclosures

Originally received: November 16, 2021.
Final revision: January 17, 2022.
Accepted: March 14, 2022.
Available online: March 18, 2022. Manuscript no. XOPS-D-21-00224

[1] The John Curtin School of Medical Research, Australian National University, Canberra, Australia.

[2] Department of Ophthalmology, Jigme Dorji Wangchuck National Referral Hospital, Ministry of Health, Royal Government of Bhutan, Thimphu, Bhutan.

[3] School of Optometry, Faculty of Health, University of Canberra, Canberra, Australia.

[4] Academic Unit of Ophthalmology, Australian National University, Canberra, Australia.

[5] Blink Eye Clinic, Canberra, Australia.

Disclosure(s):

All authors have completed and submitted the ICMJE disclosures form.

The author(s) have made the following disclosure(s): F.S.: Financial support − Diabetes Australia 2020, Alcon Australia

C.F.C.: Financial support and Royalties − Konan Medical USA, Inc; Patent (planned) − Novel analysis methods for mfPOP/OFA

J.P.v.K.: Financial support − Konan Medical USA, Inc; Patent (planned) − Novel analysis methods for mfPOP/OFA

T.M.: Financial support and Royalties − Konan Medical USA, Inc; Advisory board − EyeCo Pty Ltd., Department of Optometry, University of Canberra; Equity owner − EyeCo Pty Ltd; Nonfinancial support − Konan Medical USA, Inc.

Supported by the Rebecca L. Cooper Medical Research Fund (grant no.: PG2018040); MRFF Biotechnology Bridge (grant no.: BTBR100196), with matching funds from the Australian National University Our Health in Our Hands intramural grant; and Konan Medical USA, Inc., Irvine, California.

Presented at: The Association for Research in Vision and Ophthalmology Annual Meeting, June 2021, San Francisco, California.

HUMAN SUBJECTS: Human subjects were included in this study. The Australian National University Ethics Committee and Australian Capital Territory Health Ethics Committee approved the study. The research adhered to the tenets of the Declaration of Helsinki. All participants provided informed consent.

No animal subjects were included in this study.

AUTHOR CONTRIBUTIONS:

Concept and design: Rai, Sabeti, Carle, van Kleef, Maddess.

Data analysis and interpretation: Rai, Sabeti, Carle, van Kleef, Maddess.

Data collection: Rai, Sabeti, Carle, Rohan, van Kleef, Maddess.

Obtained Funding: Study was performed as part of regular employment duties at the Australian National University. No additional funding was provided.

Overall responsibility: Rai, Sabeti, Carle, Rohan, van Kleef, Maddess.

Abbreviations and Acronyms:
abs(DelayDiff) = delay difference; **AMD** = age-related macular degeneration; **AREDS** = Age-Related Eye Disease Study; **AUC** = area under the receiver operating characteristic curve; **BCVA** = best-corrected visual acuity; **mfPOP** = multifocal pupillographic objective perimetry; **mfVEP** = multifocal visual evoked potential; **OFA** = Objective FIELD Analyzer; **PD** = pattern deviation; **ROC** = receiver operating characteristic; **SD** = standard deviation; **TD** = total deviation.

Keywords:
ETDRS-grid OCT, macular function, multifocal pupillography, objective perimetry, rapid perimetry.

Correspondence:
Bhim Bahadur Rai, MD, PhD, Neuroscience, John Curtin School of Medical Research, Australian National University, Building 131, Garran Road, Canberra, ACT 2601, Australia. E-mail: bhim.rai@anu.edu.au.

References

1. Wong WL, Su X, Li X, et al. Global prevalence of age-related macular degeneration and disease burden projection for 2020 and 2040: a systematic review and meta-analysis. *Lancet Glob Health*. 2014;2(2):e106–e116.
2. Global Burden of Disease Blindness and Vision Impairment Collaborators. Vision Loss Expert Group of the Global Burden of Disease Study. Causes of blindness and vision impairment in 2020 and trends over 30 years, and prevalence of avoidable blindness in relation to VISION 2020: the Right to Sight: an analysis for the Global Burden of Disease Study. *Lancet Glob Health*. 2021;9(2):e144–e160.
3. Rai BB, Morley MG, Bernstein PS, Maddess T. Pattern of vitreo-retinal diseases at the national referral hospital in Bhutan: a retrospective, hospital-based study. *BMC Ophthalmol*. 2020;20(1):51.
4. Rai BB, Shresthra MK, Thapa R, et al. Pattern and presentation of vitreo-retinal diseases: an analysis of retrospective data at a tertiary eye care center in Nepal. *Asia Pac J Ophthalmol (Phila)*. 2019;8(6):481–488.
5. Kawasaki R, Yasuda M, Song SJ, et al. The prevalence of age-related macular degeneration in Asians: a systematic review and meta-analysis. *Ophthalmology*. 2010;117(5):921–927.
6. Hassell JB, Lamoureux EL, Keeffe JE. Impact of age related macular degeneration on quality of life. *Br J Ophthalmol*. 2006;90(5):593–596.
7. Sabeti F, Lane J, Rohan EMF, et al. Relationships between retinal structure and function and vision-related quality of life measures in advanced age-related macular degeneration. *Graefes Arch Clin Exp Ophthalmol*. 2021;259(12):3687–3696.
8. Sabeti F, Lane J, Rohan EMF, et al. Correlation of central versus peripheral macular structure-function with acuity in age-related macular degeneration. *Trans Vis Sci Tech*. 2021;10(2):1–10.
9. Sabeti F, Maddess T, Essex RW, et al. Multifocal pupillography in early age-related macular degeneration. *Optom Vis Sci*. 2014;91(8):904–915.
10. Gamlin PD. The pretectum: connections and oculomotor-related roles. *Prog Brain Res*. 2006;151:379–405.
11. Sabeti F, James AC, Carle CF, et al. Comparing multifocal pupillographic objective perimetry (mfPOP) and multifocal visual evoked potentials (mfVEP) in retinal diseases. *Scientific Rep*. 2017;7:45847.
12. Sabeti F, James AC, Essex RW, Maddess T. Multifocal pupillography identifies retinal dysfunction in early age-related macular degeneration. *Graefes Arch Clin Exp Ophthalmol*. 2013;251(7):1707–1716.
13. Sabeti F, Maddess T, Essex RW, James AC. Multifocal pupillography identifies ranibizumab-induced changes in retinal function for exudative age-related macular degeneration. *Invest Ophthalmol Vis Sci*. 2012;53(1):253–260.
14. Sabeti F, Maddess T, Essex RW, James AC. Multifocal pupillographic assessment of age-related macular degeneration. *Optom Vis Sci*. 2011;88(12):1477–1485.
15. Age-Related Eye Disease Study Research Group. The Age-Related Eye Disease Study system for classifying age-related macular degeneration from stereoscopic color fundus photographs: the Age-Related Eye Disease Study report number 6. *Arch Ophthalmol*. 2001;132(5):668–681.
16. Rai BB, Sabet F, Carle CF, et al. Recovery dynamics of multifocal pupillographic objective perimetry from tropicamide dilation. *Graefes Arch Clin Exp Ophthal*. 2020;258(1):191–200.
17. Maddess T, Bedford SM, Goh XL, James AC. Multifocal pupillographic visual field testing in glaucoma. *Clin Exp Ophthalmol*. 2009;30:678–686.
18. Bell A, James AC, Kolic M, et al. Dichoptic multifocal pupillography reveals afferent visual field defects in early type 2 diabetes. *Invest Ophthalmol Vis Sci*. 2010;51(1):602–608.
19. Carle CF, James AC, Maddess T. The pupillary response to color and luminance variant multifocal stimuli. *Invest Ophthalmol Vis Sci*. 2013;54:467–475.
20. Sabeti F, Nolan C, Essex R, et al. Multifocal pupillography identifies changes in visual sensitivity according to severity of diabetic retinopathy in type 2 diabetes. *Invest Ophthalmol Vis Science*. 2015;56:4504–4513.
21. Ruseckaite R, Maddess T, Danta G, et al. Sparse multifocal stimuli for the detection of multiple sclerosis. *Ann Neurol*. 2005;57(6):904–913.
22. James AC. The pattern-pulse multifocal visual evoked potential. *Invest Ophthalmol Vis Sci*. 2003;44(2):879–890.
23. James AC, Ruseckaite R, Maddess T. Effect of temporal sparseness and dichoptic presentation on multifocal visual evoked potentials. *Vis Neurosci*. 2005;22(1):45–54.
24. Carle CF, James AC, Kolic M, et al. High-resolution multifocal pupillographic objective perimetry in glaucoma. *Invest Ophthalmol Vis Sci*. 2011;52(1):604–610.
25. Won JY, Kim SE, Park YH. Effect of age and sex on retinal layer thickness and volume in normal eyes. *Medicine (Baltimore)*. 2016;95(46):e5441.
26. Pokharel A, Shrestha GS, Shrestha JB. Macular thickness and macular volume measurements using spectral domain optical coherence tomography in normal Nepalese eyes. *Clin Ophthalmol*. 2016;10:511–519.
27. Hashemi H, Khabazkhoob M, Yekta A, et al. The distribution of macular thickness and its determinants in a healthy population. *Ophthalmic Epidemiol*. 2017;24(5):323–331.
28. Wu Z, Guymer RH, Finger RP. Low luminance deficit and night vision symptoms in intermediate age-related macular degeneration. *Br J Ophthalmol*. 2016;100(3):395–398.
29. Scilley K, Jackson GR, Cideciyan AV, et al. Early age-related maculopathy and self-reported visual difficulty in daily life. *Ophthalmology*. 2002;109(7):1235–1242.
30. Steinberg JS, Fitzke FW, Fimmers R, et al. Scotopic and photopic microperimetry in patients with reticular drusen and age-related macular degeneration. *JAMA Ophthalmol*. 2015;133(6):690–697.
31. Montesano G, Ometto G, Higgins BE, et al. Structure–function analysis in macular drusen with mesopic and scotopic microperimetry. *Transl Vis Sci Technol*. 2020;9(13):43.
32. Rosli Y, Bedford SM, James AC, Maddess T. Photopic and scotopic multifocal pupillographic responses in age-related macular degeneration. *Vision Res*. 2012;69:42–48.
33. Luu CD, Dimitrov PN, Wu Z, et al. Static and flicker perimetry in age-related macular degeneration. *Invest Ophthalmol Vis Sci*. 2013;54(5):3560–3568.
34. Rai BB, Essex RW, Sabeti F, et al. An objective perimetry study of central versus peripheral sensitivities and delays in age-related macular degeneration. *Transl Vis Sci Technol*. 2021;10(14):24.
35. Rai BB, Maddess T, Carle CF, et al. Comparing objective perimetry, matrix perimetry, and regional retinal thickness in early diabetic macular oedema. *Transl Vis Sci Tech*. 2021;10(32):1–12.
36. Jansonius NM, Cervantes J, Reddikumar M, Cense B. Influence of coherence length, signal-to-noise ratio, log transform, and low-pass filtering on layer thickness assessment with OCT in the retina. *Biomed Opt Express*. 2016;7(11):4490–4500.

37. Mu Y, Zhao M, Su G. Stem cell-based therapies for age-related macular degeneration: current status and prospects. *Int J Clin Exp Med*. 2014;7(11):3843−3852.
38. Kanchanachitra C, Lindelow M, Johnston T, et al. Human resources for health in southeast Asia: shortages, distributional challenges, and international trade in health services. *Lancet*. 2011;377(9767):769−781.
39. Rai BB, Morley MG, Zangmo P, et al. Surgical management of vitreoretinal diseases in Bhutan: a 3-year national study. *New Front Ophthalmol*. 2020;6:1−6.
40. Sassmannshausen M, Steinberg JS, Fimmers R, et al. Structure-function analysis in patients with intermediate age-related macular degeneration. *Invest Ophthalmol Vis Sci*. 2018;59(3):1599−1608.
41. Sassmannshausen M, Zhou J, Pfau M, et al. Longitudinal analysis of retinal thickness and retinal function in eyes with large drusen secondary to intermediate age-related macular degeneration. *Ophthalmol Retina*. 2021;5(3):241−250.
42. Maddess T. Modeling the relative influence of fixation and sampling errors on retest variability in perimetry. *Graefes Arch Clin Exp Ophthalmol*. 2014;252(10):1611−1619.